Leukocyte, Rather than Tumor-produced SPARC, Determines Stroma and Collagen Type IV Deposition in Mammary Carcinoma

Sabina Sangaletti,[1] Antonella Stoppacciaro,[2] Cristiana Guiducci,[1] Maria Rosaria Torrisi,[2] and Mario P. Colombo[1]

[1]*Immunotherapy and Gene Therapy Unit, Department of Experimental Oncology, Istituto Nazionale per lo Studio e la Cura dei Tumori, 20133 Milan, Italy*

[2]*Department of Experimental Medicine and Pathology, Second Faculty of Medicine, University of Rome "La Sapienza," 00100 Rome, Italy*

The Journal of Experimental Medicine

Abstract

Secreted protein, acidic and rich in cysteine (SPARC), also known as osteonectin or BM-40, is a Ca^{2+}-binding matricellular glycoprotein involved in development, wound healing, and neoplasia. However, the role of SPARC in tumors is ill defined mostly because it is expressed by both tumor and stromal cells, especially inflammatory cells. We analyzed the respective roles of host- and tumor-derived SPARC in wild-type and congenic SPARC knockout ($SPARC^{-/-}$) mice on a BALB/c genetic background injected into the mammary fat pad with SPARC-producing mammary carcinoma cells derived from c-erB2 transgenic BALB/c mice. Reduced tumor growth but massive parenchyma infiltration, with large areas of necrosis and impaired vascularization were observed in $SPARC^{-/-}$ mice. Immunohistochemical analysis showed a defect in collagen type IV deposition in the stroma of lobular tumors from $SPARC^{-/-}$ mice. Chimeric mice expressing SPARC only in bone marrow–derived cells were able to organize peritumoral and perilobular stroma, whereas reciprocal chimeras transplanted with bone marrow from $SPARC^{-/-}$ mice developed tumors with less defined lobular structures, lacking assembled collagen type IV and with a parenchyma heavily infiltrated by leukocytes. Together, the data indicate that SPARC produced by host leukocytes, rather than the tumor, determines the assembly and function of tumor-associated stroma through the organization of collagen type IV.

Key words: osteonectin • extracellular matrix • leukocyte infiltration • tumor–host interactions

Introduction

Interactions between tumor and inflammatory cells represent a key issue in the complexity of neoplastic transformation and tumor progression (1, 2). Such interactions determine either tumor progression or regression through several mechanisms, including stroma formation, angiogenesis, adhesion and cell migration to and from the tumor, and cytokine and chemokine milieu, plus other factors that contribute to tissue remodeling. Emerging evidence points to host leukocytes rather than tumor cells as the source of such determining factors. This may be due simply to the availability of new tools to study leukocyte function, including mice deleted for genes encoding leukocyte-produced factors. Indeed, KO mice provide a direct means to examine the in vivo molecular events responsible for neoplastic transformation. The importance of inflammatory cytokines in determining the tumor microenvironment has been underlined by the findings that TNFα KO mice are resistant to skin carcinogenesis (3), whereas those lacking IL-1β are resistant to the development of experimental metastases (4). Furthermore, *op/op* mice, which are naturally deficient in CSF-1 (5, 6), show impaired tumor growth (7) and progression (8). Matrix metalloproteinase (MMP)-9 has been shown to be required for progression of skin carcinogenesis, and bone marrow transplantation (BMT) experiments have demonstrated that leukocytes are the critical source of MMP-9 in the tumor environment

The online version of this article includes supplemental material.

Address correspondence to Mario P. Colombo, Immunotherapy and Gene Therapy Unit, Istituto Nazionale Tumori, Via Venezian 1, 20133 Milan, Italy. Phone: 39-02-2390-2252; Fax: 39-02-2390-2630; email: mcolombo@istitutotumori.mi.it

Abbreviations used in this paper: BMT, bone marrow transplantation; ECM, extracellular matrix; MMP, matrix metalloproteinase; PECAM-1, platelet–endothelial cell adhesion molecule 1; SPARC, secreted protein, acidic and rich in cysteine.

 J. Exp. Med. © The Rockefeller University Press • 0022-1007/2003/11/1475/11 $8.00
Volume 198, Number 10, November 17, 2003 1475–1485
http://www.jem.org/cgi/doi/10.1084/jem.20030202

(9). MMP-9 produced by host macrophages has also been shown to promote outgrowth of human ovarian carcinoma xenotransplanted into *nu/nu* mice (10).

In this work, we used a KO mouse model to analyze the role of a potentially regulatory matricellular protein in tumor–host interactions. Secreted protein, acidic and rich in cysteine (SPARC), also known as osteonectin or BM-40, is a Ca^{2+}-binding matricellular glycoprotein that binds to a range of extracellular matrix (ECM) components such as thrombospondin-I (11), vitronectin (12), fibrillar collagen (types I, II, III, and V), and collagen type IV (13, 14), the predominant structural component of the basement membrane. SPARC is expressed during development and, in adults, during processes requiring ECM turnover such as wound healing and tumor progression. The amino acid sequence of SPARC is highly conserved among species from *Drosophila melanogaster* (15) to humans (16). A variety of in vitro papers have suggested a role for SPARC in the regulation of cell adhesion and proliferation, and in the modulation of cytokine activity (17–20). Although SPARC expression appears to be deregulated in transformed cells (21–23), its inhibition by antisense RNA diminished both the adhesive and invasive capacities of human melanoma cells in vitro and in xenotransplanted *nu/nu* mice (24). The role of SPARC in neoplastic cell transformation, conditioning inflammation, and leukocyte trafficking has not been well defined in vivo, where the major phenotypes reported so far in SPARC KO mice are cataract formation (25–27) and osteopenia (28, 29). The former is associated with an altered collagen type IV protein (30).

To obtain $SPARC^{-/-}$ mice on a genetic background suitable for tissue transplantation and immunological studies, we backcrossed SPARC KO mice (26) that were originally on a mixed 129 background to BALB/c mice, followed by interbreeding to obtain a congenic BALB/c/$SPARC^{-/-}$ strain that retains the original phenotype described in 129 mice (unpublished data). We also backcrossed outbred mice transgenically expressing the rat oncogene c-erB2 (HER-2/neu) driven by the mouse mammary tumor virus promoter to BALB/c mice. Female mice carrying the activated rat HER-2/neu oncogene present high numbers of breast tumor nodules characterized as lobular carcinomas with lobes defined by connective septa containing collagen type IV (31). The onset of mammary gland hyperplasia and carcinoma have been carefully characterized in these transgenic mice (32), which were used as the source of mammary carcinomas and cell lines in the present work.

We evaluated the role of tumor-derived SPARC in stroma formation and tumor outgrowth in wild-type and congenic $SPARC^{-/-}$ mice injected with SPARC-producing mammary carcinoma cells. We also analyzed the role of leukocyte-produced SPARC, using chimeric mice expressing SPARC only in donor BM-derived cells. Our results revealed impairment of growth, vascularization, and stroma formation in tumors implanted into $SPARC^{-/-}$ mice. Reduced lobular structure and intervening stroma in the absence of host-produced SPARC were associated with reduced collagen type IV deposition, an event that might favor leukocyte infiltration of tumor parenchyma. This phenotype was reversed by transplanting BM from $SPARC^{+/+}$ donors. Thus, the organization of tumor stroma depends on SPARC produced by host leukocytes rather than on tumor-derived SPARC.

Materials and Methods

Mice and Tumors. SPARC KO mice on a mixed 129SV/C57BL/6 background (26) were provided by C. Howe (The Wistar Institute, Philadelphia, PA). Mice were backcrossed for 12 generations with BALB/cAnNCrl (Charles River Laboratories) to obtain congenic $SPARC^{-/-}$ mice. Heterozygous and homozygous animals were identified by Southern blot analysis using the 280-bp HindIII-BamHI fragment of SPARC cDNA as a probe. Mouse tail DNA was digested with restriction enzyme NSII to distinguish the wild-type gene (5.3-kb fragment) from the KO gene (7.9-kb fragment).

Female BALB-neuT mice are transgenic for the activated form of the rat c-erB2 oncogene and develop mammary tumors involving all mammary glands (32). Mice were bred and maintained at the Istituto Nazionale Tumori under standard conditions according to institutional guidelines.

N1G, N2C (thoracic), and N3D (inguinal) primary mammary carcinoma cell lines were derived from female BALB-neuT mice. Tumors were removed and, in a sterile environment, cleaned of fat, large vessels, and necrotic areas, minced with scissors, and placed in warm trypsin (37°C for 30 min). After washing with DMEM (Bio Whittaker) and the addition of 10% heat-inactivated FCS (Bio Whittaker), tissue was passed through strainers and washed again. Cells were counted and seeded in 6-well plates at 0.4×10^6 cells/ml in DMEM plus 20% FCS. Tumorigenicity of carcinoma cells was assayed in wild-type, $SPARC^{-/-}$, and chimeric mice injected s.c. into the mammary fat of the inguinal region with the cells at a predetermined minimal lethal dose. Tumor take and volume were monitored twice per week. Tumors were measured with calipers in the two perpendicular diameters, and tumor volume (mm^3) was calculated as long diameter × short diameter^2.

Morphological Analysis and Immunohistochemistry. For histological evaluation, tumor fragments were fixed in 10% neutral-buffered formalin, embedded in paraffin, sectioned (5 μm), and stained with hematoxylin and eosin (H&E) or Masson's trichrome. H&E-stained sections showed that the transplanted tumors are similar to the primary neoplasia (31). Cancer cells grew in solid nests forming lobules and less frequently ductular structures endowed with dense, well-vascularized, connective tissue.

For immunohistology, tumor fragments were embedded in OCT compound, snap frozen, and stored at −80°C. For immunohistochemical analysis, 5-μm cryostat sections were fixed in acetone and incubated for 1 h with the following: (a) mouse anti-osteonectin mAb (clone ON1–1; Takara Biomedicals); (b) rabbit polyclonal Ab against mouse collagen type IV (AB756; Chemicon); (c) rabbit anti–mouse collagen type I (Biodesign International); (d) rat anti–mouse mAb CD31 (platelet–endothelial cell adhesion molecule 1 [PECAM-1]); (e) biotinylated rat mAb against mouse CD45 (clone 30-F11) and Ly-6G (clone RB6–8C5); (f) fluorescein-isothiocyanate (FITC)-conjugated mAbs against CD11c (clone HL3), CD11b (clone MI/70), CD4 (clone GK 1.5; all from BD Biosciences); and (g) F4/80 (clone CI: A3–1;

Caltag). After washing, sections were sequentially overlaid with biotinylated goat anti–rabbit IgG for 30 min and with avidin–peroxidase complex for 30 min (Sigma-Aldrich). Avidin–peroxidase complex or peroxidase-conjugated rabbit anti-FITC antibody (DakoCytomation) was used as secondary antibody for sections incubated with biotinylated primary antibodies or FITC-conjugated primary antibody, respectively. Antigen was revealed with 3,3′-diaminobenzidine (Sigma-Aldrich) according to the manufacturer's instructions. Sections were counterstained with Mayer's hematoxylin, dehydrated in graded alcohol (70, 95, and 100% ethanol), and mounted in BDH mounting medium (Merck Eurolabs). All immunolocalization experiments were repeated three times with multiple sections, including negative controls for determination of background staining. All images were digitally captured on a microscope (Nikon) equipped with a digital camera (DXM1200; Nikon) and analyzed using ACT1 software. The number of microvessels and immunostained cells was determined by light microscopy at 400 magnification in 10 fields on a 1-mm^2 grid and is given as cells/mm^2 (mean ± SD).

In Situ Hybridization. The presence of cytokine mRNA was investigated by in situ hybridization using TNFα and IFNγ cDNA probes (33). Each specific probe (1 μg) was labeled with biotin using the Renaissance Random Primer Labeling Kit (NEN Life Science Products).

Cryostat sections were processed for in situ hybridization as described previously (33) except for probe detection. In brief, slides were air dried, rehydrated in PBS, blocked with 10% FCS in PBS, incubated with avidin–peroxidase complex for 30 min, and washed. Reactivity was revealed with 3,3′-diaminobenzidine followed by Mayer's hematoxylin counterstaining. Pst-1–digested pUC9 plasmid fragments were used in negative control sections.

Treatment of SPARC$^{+/+}$ and Congenic SPARC$^{-/-}$ Mice with Anti-TNFα and -INFγ Neutralizing mAbs. SPARC$^{+/+}$ and SPARC$^{-/-}$ mice were injected s.c. with N2C mammary carcinoma cells at the minimal lethal dose and treated with 200 μg of anti-TNFα (V1Q hybridoma, provided by D. Mannell, University of Regensburg, Regensburg, Germany) and 200 μg of anti-IFNγ (AN18 hybridoma, provided by G. Garotta, Roche, Basel, Switzerland) mAb twice weekly starting on day 1 after tumor injection. Tumor take and volume were monitored twice per week.

BMT. SPARC$^{+/+}$ and SPARC$^{-/-}$ mice on a BALB/c background were lethally γ irradiated with 900 cGy (given as a split dose 450 + 450 cGy with a 3-h interval between the first and the second irradiation), whereas CB6F1 (SPARC$^{+/+}$) mice received a total of 950 cGy (500 + 450). 2 h later, mice were injected i.v. with 2 × 10^7-nucleated cells obtained from SPARC$^{+/+}$ or SPARC$^{-/-}$ donors as follows. BM-derived cells were obtained by flushing the cavity of freshly dissected femurs with saline. Flushed cells were dispersed by pipetting across strainers, washed, and resuspended in saline. Recipient mice received 0.4 mg/ml gentalyn added to the drinking water starting 1 wk before irradiation and maintained thereafter. To verify engraftment, PBMCs withdrawn from the retro-orbital sinus at 4, 6, and 8 wk after BMT were stained with FITC-conjugated mouse anti–mouse H-2K^b and PE-conjugated mouse anti–mouse H-2K^d, as well as isotype control FITC- and PE-conjugated mouse IgG2a, and analyzed by cytofluorimetry. A total of 5,000-gated events were collected on a FACScan™ (Becton Dickinson) and analyzed using CELLQuest™ software (Becton Dickinson). At 8 wk after BMT, chimeric mice were injected s.c. with 5 × 10^5 N2C tumor cells.

RNA and Northern Blot Analysis. Total RNA was extracted from N1G, N2C, and N3D cells using TRIzol (Promega) and aliquots (10 μg) were run on a 1.0% agarose-formaldehyde gel,

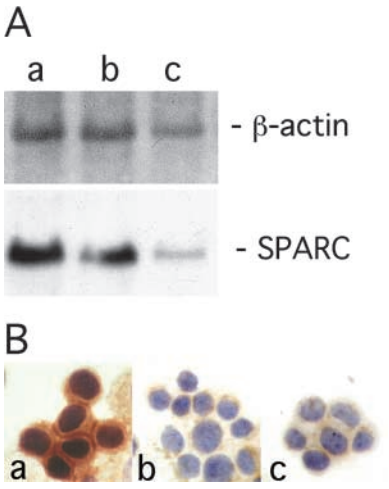

Figure 1. SPARC expression in primary mammary carcinoma cell lines. Northern blotting (A) and immunohistochemical (B) analysis of N2C (a), N1G (b), and N3D (c) cell lines. Northern blot analysis was performed by sequential hybridization with SPARC and β-actin probes. SPARC staining localized in the cytoplasm of all three cell lines, but the higher amount of SPARC produced by N2C appeared to show an apparent staining of the nuclei, which are normally negative.

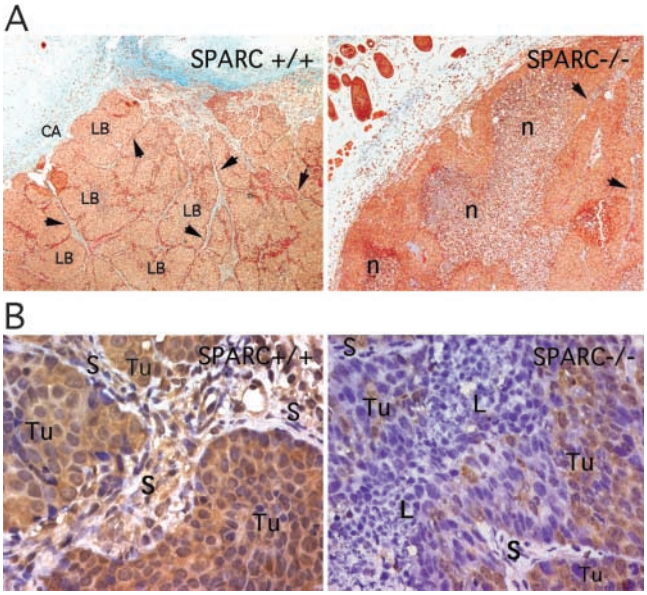

Figure 2. Histological features and SPARC expression of N2C tumors in SPARC$^{+/+}$ and SPARC$^{-/-}$ mice. (A) N2C tumors grew in SPARC$^{+/+}$ mice as solid nests forming lobules (LB) embedded in dense, well-vascularized, connective tissue (arrowheads) and surrounded by a well-defined connective capsule (CA). Tumors from SPARC$^{-/-}$ mice were smaller and histologically characterized by less defined lobules, not completely surrounded by the stromal septa (arrowheads) and frequently presenting necrotic (n) areas. Original magnification, 40. (B) N2C tumor cells grown in SPARC$^{+/+}$ or SPARC$^{-/-}$ mice produced SPARC as detected immunohistochemically with anti-SPARC mAbs. In the SPARC$^{+/+}$ host, all of the cells (tumor [Tu] and stromal [S]) were strongly reactive. In the SPARC$^{-/-}$ host, only the tumor cells (Tu) were positive for SPARC expression, whereas the massive leukocyte infiltrate (L) invading one septum, as well as stromal cells (S) in the thin connective septa, were completely negative. Formalin fixed, paraffin embedded sections are shown. Original magnification, 200.

transferred onto a nylon membrane (Hybond-N; Amersham Biosciences) by Northern blotting. Hybridization was performed with the 571-bp EcoRI fragment of mouse SPARC cDNA labeled with α-[^{32}P]-dCTP using the Multiprime labeling kit (Amersham Biosciences) in the presence of 50% formamide and 10% dextran sulfate. Filters were washed at high stringency (0.2× SSC, 0.1% SDS at 55°C for 2 h) and exposed to film for 16–48 h at −70°C (X-AR5; Kodak).

Online Supplemental Material. Fig. S1 shows immunostaining of collagen type I and collagen type IV in tumors from SPARC$^{+/+}$ mice. Fig. S2 shows collagen deposition (Masson's trichrome and immunostaining) in tumors from SPARC$^{+/+}$ > SPARC$^{-/-}$ and SPARC$^{-/-}$ > SPARC$^{+/+}$ chimeras. Fig. S3 shows in vitro migration of macrophages from SPARC$^{+/+}$ and SPARC$^{-/-}$ mice in response to Mip-1α. Fig. S4 shows leukocyte infiltration in the ears of SPARC$^{+/+}$ and SPARC$^{-/-}$ mice after phorbol ester–induced inflammation. Online supplemental material is available at http://www.jem.org/cgi/content/full/jem.20030202/DC1.

Results

Impaired Tumor Stroma and Defective Collagen Type IV Deposition in the Absence of Host-produced SPARC. Thoracic- and inguinal-transformed mammary glands were collected from Her2neu transgenic BALB-neuT mice. Half of each primary tumor nodule was used to establish cell lines, whereas the other half was used for in vivo passages as trocar pieces. Carcinoma cell lines N2C, N1G, and N3D were characterized for SPARC expression by Northern blot analysis and immunostaining.

N2C cells expressing the highest level of tumor-derived SPARC (Fig. 1) were selected for injection into SPARC$^{+/+}$ and SPARC$^{-/-}$ mice. Compared with tumors from wild-type mice, those from SPARC$^{-/-}$ mice were smaller and histologically characterized by undefined lobules, frequently presenting necrotic central areas (Fig. 2 A). The lobules were not completely delineated by the stromal septa, which appeared generally thin (Fig. 2 A) and sometimes heavily infiltrated by leukocytes (Fig. 2 B). Anti-SPARC staining of tumor cells in vivo was detectable in both host types (Fig. 2 B), and staining intensity was indistinguishable from that in primary tumors passed directly in vivo as trocar pieces (not depicted). Unlike tumors implanted into SPARC$^{+/+}$ mice, those in SPARC$^{-/-}$ mice revealed no SPARC expression in the stromal compartment or in infiltrating leukocytes (Fig. 2 B). The Masson's trichrome staining revealed an overall reduction of collagen in tumors from SPARC$^{-/-}$ as compared with those of the same volume from SPARC$^{+/+}$ mice. The collagen was nearly absent at the growing edge of the SPARC$^{-/-}$ tumor and was strongly reduced in the intratumor connective septa (Fig. 3, top). Immunostaining showed that collagen type IV was the predominant stromal component of lobular tumors from SPARC$^{+/+}$ mice, whereas tumors from SPARC$^{-/-}$ mice revealed a general absence of collagen type IV positive structures, such as the basement membrane of tumor lobules or vessels either within or at the tumor edge (Fig. 3, middle). Collagen IV residual staining was associated with the cytoplasm of some stromal cells and with the basement membrane of few resi-

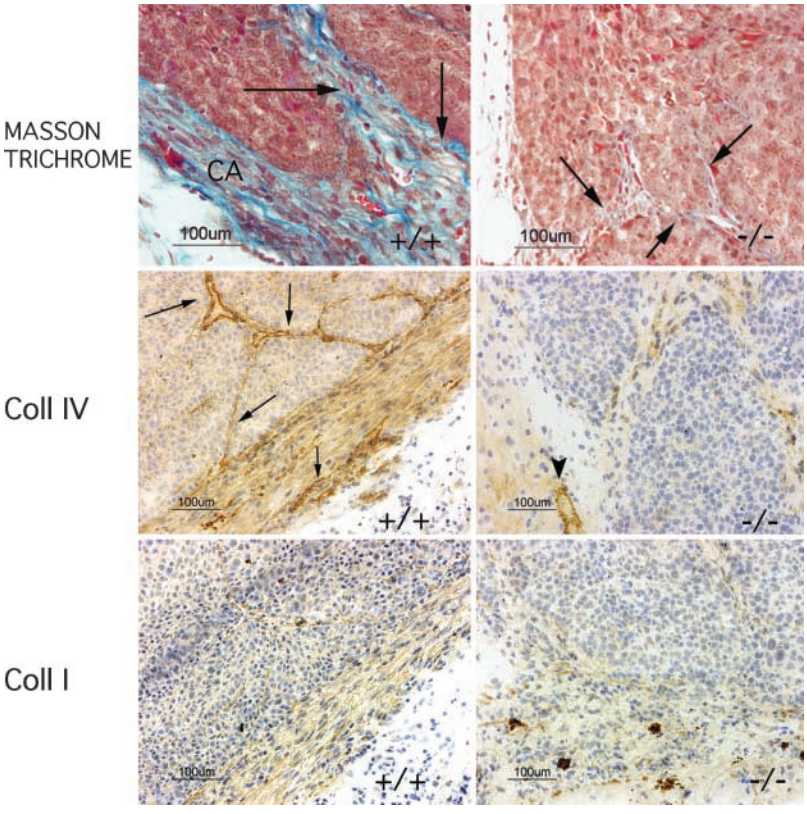

Figure 3. N2C tumors in SPARC$^{-/-}$ mice show a defect in collagen deposition. Representative serial sections of N2C tumors grown s.c. in SPARC$^{+/+}$ and SPARC$^{-/-}$ mice and stained with Masson's trichrome (top) and immunostained for collagen type IV (middle, Coll IV) or collagen type I (bottom, Coll I). Masson's trichrome revealed decreased collagen in the stroma of tumors from SPARC$^{-/-}$ mice, both at the periphery (CA, capsular area in SPARC$^{+/+}$ mice) and in the connective tissue septa (arrows). Collagen type IV staining defined basement membrane structures localizing at the level of vessels and connective septa (arrows) in the wild-type mice. Collagen type IV also accounted for most of the collagen in the capsular area, where collagen type I staining was less intense. In tumors from SPARC$^{-/-}$ mice, the poor collagen type IV deposition did not serve to define septa or the peripheral stroma; only the basement membrane of a preexisting vessel outside the tumor area showed staining for collagen type IV (arrowhead).

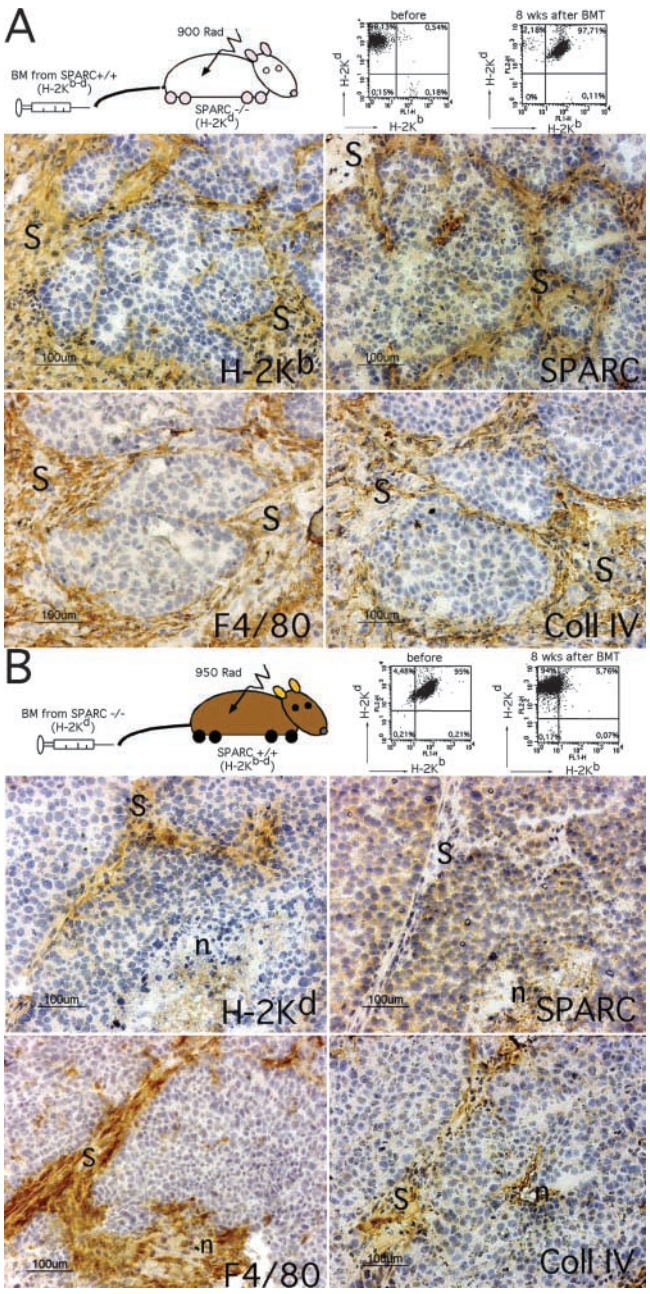

Figure 4. Stroma deposition in tumors from chimeric mice. SPARC$^{+/+}$ (CB6F1, H-2^{bd}) > SPARC$^{-/-}$ (BALB/c, H-2^{d}) chimeric mice (A) and reciprocal chimeras SPARC$^{-/-}$ (BALB/c, H-2^{d}) > SPARC$^{+/+}$ (CB6F1, H-2^{b-d}) mice (B) were injected s.c. with N2C tumor cells 8 wk after BMT. BMT design for each type of chimera and expression of donor MHC class I antigens in PBMCs of transplanted mice before and after BMT are shown above each panel. Cryostat sections of tumors were stained for MHC-I donor antigen, macrophages (F4/80), SPARC, and collagen type IV. In SPARC$^{+/+}$ > SPARC$^{-/-}$ chimeras, donor (H-2K^{b}) SPARC-producing macrophages (F4/80^{+}) represent the major cellular component of the stroma (S) and colocalize with a bright staining of collagen type IV. However, in tumors from SPARC$^{-/-}$ > SPARC$^{+/+}$ chimeras, macrophages recruited from donor BM are unable to produce SPARC and are associated with reduced collagen type IV. In these tumors, necrotic (n) areas are as frequent as in tumors from SPARC$^{-/-}$ mice.

dent vessels (Fig. 3, middle). A structural vessel outside the tumor area, and likely not undergoing remodeling, stains strongly for collagen type IV (Fig. 3, arrowheads). Collagen type I was almost exclusively localized at the periphery of tumors from SPARC$^{+/+}$ mice and its immunostaining was less intense in tumors from SPARC$^{-/-}$ mice (Fig. 3, bottom). The distinct specificity of Abs to collagens types I and IV was confirmed by double immunostaining (Fig. S1, available at http://www.jem.org/cgi/content/full/jem.20030202/DC1).

To test whether the lack of SPARC by tumor-associated host leukocytes accounted for impaired stroma formation, SPARC$^{-/-}$ mice were lethally irradiated and transplanted with BM from CB6F1 (SPARC$^{+/+}$) mice before injection with N2C carcinoma cells. In the presence of SPARC-producing donor leukocytes, stroma appeared identical to that of N2C tumors grown in SPARC$^{+/+}$ mice; however, tumors from reciprocal chimeras in which BM of SPARC$^{-/-}$ donors transplanted into SPARC$^{+/+}$ (CB6F1) recipients showed the same reduced stroma and impaired collagen deposition seen in SPARC$^{-/-}$ mice (Fig. 4 and Fig. S2, A and B available at http://www.jem.org/cgi/content/full/jem.20030202/DC1). In particular, serial sections of N2C tumor s.c. grown in SPARC$^{+/+}$ > SPARC$^{-/-}$ chimeras revealed donor (H-2K^{b}) SPARC-producing macrophages (F4/80^{+}), accounting for the major cellular component of the stroma and colocalizing with a bright staining of collagen type IV (Fig. 4 A). In reciprocal SPARC$^{-/-}$ > SPARC$^{+/+}$ chimeras in which BM of SPARC$^{-/-}$ donors was transplanted into SPARC$^{+/+}$ (CB6F1) recipients, donor take was judged based on loss of H-2K^{b} expression in PBMCs; thus, tumor sections could only be stained with H-2K^{d} (common to host and donor). Because the tumors expressed low levels of H-2K^{d}, which were undetectable by immunohistochemistry, only stromal cells were decorated by the H-2K^{d} mAb. Most of those stromal cells also stain for F4/80 in areas of weak, residual collagen type IV staining, confirming that in tumors from SPARC$^{-/-}$ > SPARC$^{+/+}$ chimeras, macrophages recruited from donor BM are unable to produce SPARC and are associated with reduced collagen type IV (Fig. 4 B).

Correlation between Tumorigenicity and Leukocyte Infiltration. Because stroma formation appeared to depend on SPARC produced by leukocytes, we analyzed the extent of leukocyte infiltration and its possible influence on the outgrowth of transplanted tumors in SPARC$^{+/+}$ and SPARC$^{-/-}$ mice. The total leukocyte population that was immunostained using mAb to CD45 was significantly larger in tumors from both SPARC$^{-/-}$ mice and mice receiving BM from SPARC$^{-/-}$ donors than in tumors from SPARC$^{+/+}$ and SPARC$^{+/+}$ > SPARC$^{-/-}$ chimeras (Fig. 5, A and B). Although leukocytes in tumors from SPARC$^{+/+}$ mice localized in the perilobular stroma, those in tumors from SPARC$^{-/-}$ mice were more dispersed, with some deeply infiltrating the tumor parenchyma (Fig. 5 B), but mostly associated to necrotic areas (Fig. 6) or with some areas of less defined perilobular septa.

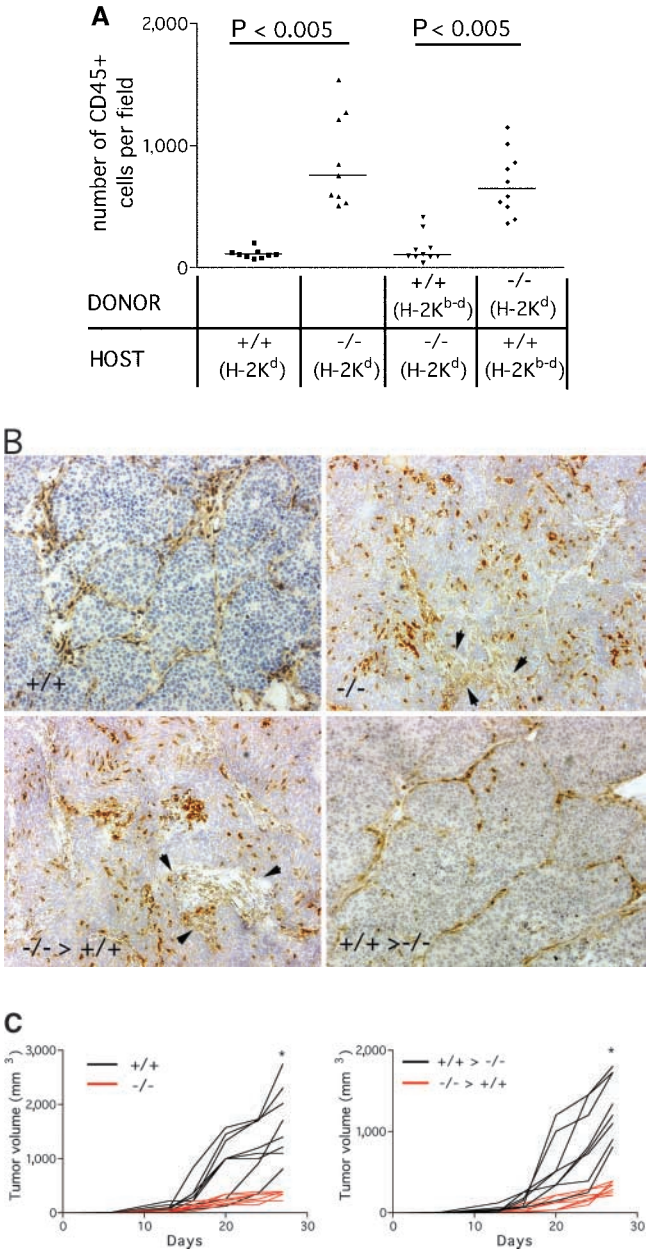

Figure 5. Tumorigenicity of N2C cells is inversely correlated with the number of infiltrating leukocytes. Cryostat sections of tumor from SPARC$^{+/+}$, SPARC$^{-/-}$, SPARC$^{+/+}$ > SPARC$^{-/-}$, and SPARC$^{-/-}$ > SPARC$^{+/+}$ chimeric mice were immunostained for the common leukocyte antigen CD45. Quantitative analysis of CD45^{+} cells (A) revealed significantly (Student's *t* test) higher number of CD45^{+} cells in tumors from SPARC$^{-/-}$ and SPARC$^{-/-}$ > SPARC$^{+/+}$ chimeric mice (−/− > +/+) as compared with tumors from SPARC$^{+/+}$ mice and SPARC$^{+/+}$ > SPARC$^{-/-}$ chimeras (+/+ > −/−). (B) Localization of CD45^{+} cells within the tumors. In wild-type and chimeric SPARC$^{+/+}$ > SPARC$^{-/-}$ mice, CD45^{+} cells were localized mainly in the connective septa completely defining lobular structures, with only a few cells infiltrating the tumor parenchyma. In tumors from SPARC$^{-/-}$ mice and SPARC$^{-/-}$ > SPARC$^{+/+}$ chimeras, CD45^{+} cells were distributed in the residual septa, which were sometimes completely infiltrated by these cells (arrowheads) but also localized within the tumor parenchyma. Analysis of N2C tumor growth kinetics (C) showed that growth was impaired in SPARC$^{-/-}$ and SPARC$^{-/-}$ > SPARC$^{+/+}$ chimeras as compared with wild-type and SPARC$^{+/+}$ > SPARC$^{-/-}$ mice (*, $P < 0.005$; Student's *t* test at day 27). Original magnification, 100.

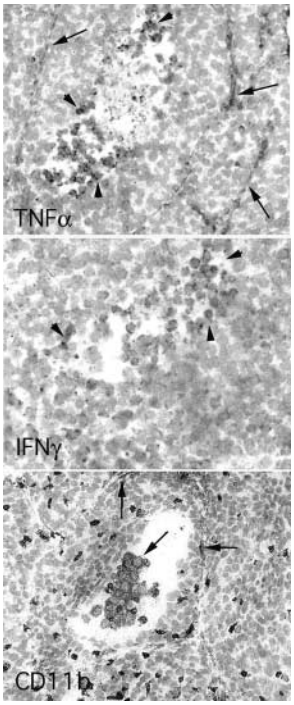

Figure 6. Expression of TNFα and IFNγ in tumors N2C from SPARC$^{-/-}$ mice. In situ hybridization analysis revealed expression of TNFα mRNA both in stromal cells (arrows) and cells localized within a necrotic area (arrowheads), whereas IFNγ was detected only in cells within the necrotic area. Cells localizing in the necrotic area stained with mAb to CD11b, which defines granulocytes and macrophages.

Analysis of N2C tumor growth kinetics revealed significantly reduced outgrowth in SPARC$^{-/-}$ and SPARC$^{-/-}$ > SPARC$^{+/+}$ chimeric mice (i.e., the lines with the highest number of infiltrating leukocytes, as compared with tumors from SPARC$^{+/+}$, SPARC$^{+/+}$ > SPARC$^{-/-}$ [Fig. 5 C] and control chimeric mice [not depicted]). Thus, in the absence of SPARC, leukocytes might infiltrate the tumor more easily and may counter tumor growth.

Characterization of Infiltrating Leukocytes. Immunostaining with Abs to various leukocyte subpopulations indicated that all leukocyte types were more abundant in tumors from SPARC$^{-/-}$ than SPARC$^{+/+}$ mice (Table I). CD11b^{+} staining, which detects both macrophages and granulocytes, is abundant around the large area of necrosis that characterizes tumors from SPARC$^{-/-}$ mice (Fig. 6 and not depicted).

In situ hybridization revealed expression of TNFα and, to a lesser extent, IFNγ mRNA in infiltrating cells around and within necrotic areas of the SPARC$^{-/-}$ mouse tumors

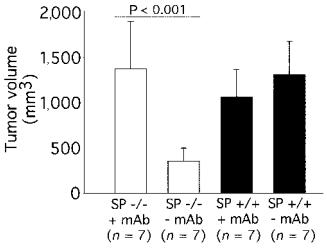

Figure 7. Enhanced tumor growth in SPARC$^{-/-}$ mice treated with neutralizing antibodies against TNFα and IFNγ. Mean ± SD final volume of N2C tumors was compared 22 d after s.c. injection into SPARC$^{+/+}$ and SPARC$^{-/-}$ mice treated i.p. with 200 μg of mAb against both TNFα and IFNγ starting 1 d after tumor cell injection. Results are from one experiment of three performed. P-value was determined by Student's *t* test.

Table I. *Profile of Leukocytes Infiltrating Tumors from SPARC$^{+/+}$ and SPARC$^{-/-}$ Mice*

	F4/80	CD11b	Ly-6G	CD11c	CD4	CD8
SPARC $^{+/+}$	176.9 ± 74.5[a]	147.0 ± 136.1	32.7 ± 11.2	68.8 ± 43.4	43.7 ± 45.0	1.4 ± 2
SPARC$^{-/-}$	564.5 ± 287.8	545 ± 129	130.4 ± 70.0	328.0 ± 128.0	146.0 ± 95.9	14.0 ± 5.6

Data are from five mice for both SPARC$^{+/+}$ and SPARC$^{-/-}$ mice. For each sample, 10 randomly chosen fields were analyzed, and the data were compared using Student's *t* test. $P < 0.005$ for all groups.
[a]Mean number of cells/mm^2 (±SD) positive for immunostaining.

(Fig. 6). TNFα was also expressed in cells localized in the thin stroma delimiting the less organized lobular structures. To test the potential role of these cytokines in the reduced growth of N2C tumors in SPARC$^{-/-}$ as compared with SPARC$^{+/+}$ mice, tumor outgrowth was monitored in mice treated twice per week with neutralizing mAb against TNFα and IFNγ starting 1 d after the N2C cell injection. Tumor growth was significantly ($P < 0.001$) accelerated in SPARC$^{-/-}$ mice with respect to control untreated SPARC$^{-/-}$ mice, whereas tumor growth was similar in treated versus untreated SPARC$^{+/+}$ mice (Fig. 7). Indeed, in antibody-treated SPARC$^{-/-}$ mice, N2C tumor growth was similar to that observed in SPARC$^{+/+}$ mice.

Impaired Vascular Supply in N2C Tumors from SPARC$^{-/-}$ Mice. Reduced mammary tumor growth might reflect reduced nutrient and/or cytokine supply related to impaired peritumoral stroma (34). Analysis of vascularization based on PECAM-1 (CD31) immunostaining in the peritumoral and perilobular stroma from SPARC$^{-/-}$ and SPARC$^{+/+}$ mice revealed small and few vessels supplying tumors from SPARC$^{-/-}$ mice, as compared with the highly vascularized tumors from SPARC$^{+/+}$ mice (Fig. 8). Calculation of the vascularized (CD31$^+$) area relative to that of tumors in SPARC$^{-/-}$ and SPARC$^{+/+}$ mice (five mice in each group; 10 observations per mouse in defined tumor area) indicated a significantly ($P < 0.005$) smaller vascularized area in tumors from SPARC$^{-/-}$ mice (4.7 ± 1.9% vs. 11.9 ± 5.5%).

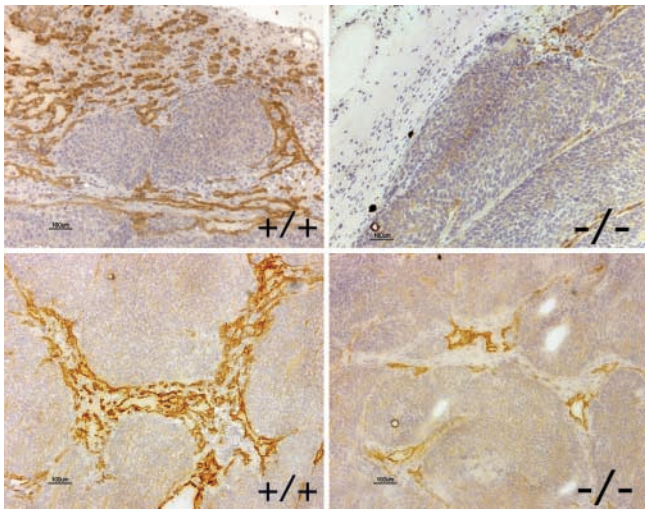

Figure 8. Immunohistochemical characterization of blood vessels associated with N2C tumors from SPARC$^{+/+}$ and SPARC$^{-/-}$ mice. N2C tumor obtained from SPARC$^{+/+}$ and SPARC$^{-/-}$ mice were immunostained with mAbs against CD31/PECAM-1 to characterize tumor-associated blood vessels. Although tumors from SPARC$^{+/+}$ mice were highly vascularized, those from SPARC$^{-/-}$ mice showed a dramatic reduction in number and size of tumor-associated blood vessels both at the periphery (top; original magnification, 100) and inside the tumor (bottom; original magnification, 200).

Discussion

SPARC has been implicated in tumor–host interactions by virtue of its ability to bind several matrix components, such as thrombospondin-1, vitronectin, fibrillar collagen, and collagen type IV. This notion is strengthened by the observation that SPARC expression is associated with tissues undergoing repair, remodeling, and turnover (for review see reference 14). However, the precise role of SPARC in tumorigenesis and tumor progression has remained unclear because of disparate results in numerous papers. In ovarian carcinomas, SPARC down-regulation has been associated with tumor progression because it is expressed in normal ovary cells and gradually lost as disease progresses (35, 36). Moreover, restoration of SPARC expression in ovarian carcinoma cells by gene transduction suppresses tumorigenesis by inducing apoptosis (37). Similar growth suppression has been reported for human breast cancer cells induced to express SPARC by treatment with doxicyclin (38). By contrast, SPARC has protumoral activity in other tumor cell types. For example, SPARC inhibition by antisense oligonucleotides reduced tumorigenicity of melanoma cell lines in nude mice, and melanoma cell clones with the lowest expression of SPARC lost the ability to adhere (25), an ability required for eventual invasion. Moreover, glioma cell lines transfected to express different amounts of SPARC acquire an increasingly malignant phenotype as a function of increased SPARC expression (39–41).

Although tissue variation might explain the conflicting results, an added complexity stems from the fact that both tumor and stroma cells can produce SPARC. In the present work, we developed a mouse model that allowed dissection of the role of SPARC produced by BM-derived inflammatory cells from that of SPARC-producing tumor cells.

When injected into SPARC$^{+/+}$ mice, the BALB-neuT–derived N2C, N1G, and N3D mammary carcinoma cell lines grew as a solid tumor characterized by a well-structured stroma comprised predominantly of macrophages and of collagen type IV defining the lobular structure of these tumors. The same tumors grown in congenic SPARC$^{-/-}$ mice showed a clear defect in matrix assembly that was not due to impaired recruitment of stroma cell components but rather to a defect in deposition of collagen type IV. Altered collagen type IV deposition has been detected in the specialized ECM that forms the lens capsule (28) in SPARC$^{-/-}$ mice. Our results indicate that alteration of collagen type IV assembly is a more general defect associated with a SPARC deficit.

To better illustrate the distinct role of host-versus-tumor–produced SPARC, most of our experiments were performed using the N2C cell line, the highest SPARC producer, and using BM chimeras, in which SPARC production derives from cells of BM origin. Our analysis of tumor matrix assembly in SPARC$^{-/-}$ > SPARC$^{+/+}$, reciprocal SPARC$^{+/+}$ > SPARC$^{-/-}$, and control chimeric mice injected with N2C cells 8 wk after BMT revealed defective collagen, mainly type IV, only in mice receiving BM from SPARC$^{-/-}$ donors. This finding demonstrates the crucial role of SPARC produced by BM-derived cells in collagen type IV assembly in the tumor environment, and the inability of tumor-produced SPARC to substitute that from leukocytes in organizing the intervening stroma defining lobular structures of this mammary carcinoma. Our results add a matricellular protein to the list of factors that, when produced by inflammatory cells, can promote malignant outgrowth rather than normal development (for review see references 1, 2).

We investigated whether impaired matrix formation in tumors from SPARC$^{-/-}$ mice has any functional significance for leukocyte migration. Migration of T lymphocytes through basement membrane has been shown to require MMP-9 secretion (42), and T cell homing to extravascular sites requires penetration of the subendothelial lamina, a specialized connective tissue formed by collagen types IV and V (43). Migration of Langerhans cells from the skin to draining lymph nodes also requires MMPs to cleave collagen fibers that hamper cell migration (44). The same has been described for macrophages invading tissues (10). Thus, a less organized stroma is expected to favor cell migration and, therefore, leukocyte infiltration. The parenchyma of tumors from SPARC$^{-/-}$ and SPARC$^{-/-}$ > SPARC$^{+/+}$ chimeric mice were infiltrated by a large number of CD45^{+} leukocytes further identified as macrophages (CD11b^{+} and F4/80^{+}), granulocytes (CD11b^{+} and Ly6G^{+}), and less numerous lymphocytes (CD4^{+}) and dendritic cells (CD11c^{+}). N2C tumors from SPARC$^{+/+}$ > SPARC$^{-/-}$ chimeras were infiltrated with macrophages only bordering tumor lobes as part of the structural stroma. Such different patterns of leukocyte infiltration are not due to a differential intrinsic migratory capacity of cells from SPARC$^{-/-}$ and SPARC$^{+/+}$ mice, because macrophages (Fig. S3, available at http://www.jem.org/cgi/content/full/jem.20030202/DC1) and dendritic cells (not depicted) from the two mouse strains migrate equally well in vitro in response to MIP-1α and MIP-3α, respectively. The more extensive CD45^{+} cell infiltration of inflamed tissue, such as mouse ear skin treated with TPA in SPARC$^{-/-}$ than in SPARC$^{+/+}$ mice (Fig. S4, available at http://www.jem.org/cgi/content/full/jem.20030202/DC1), is consistent with a role of SPARC in leukocytes migration in vivo.

TGFβ is reportedly down-regulated in absence of SPARC (45), and Hazelbag et al. (46) found a direct correlation between increased TGFβ expression, increased collagen type IV production, and reduced leukocyte infiltration in cervical cancer, a result that mirrors our findings in which the absence of SPARC correlated with low collagen type IV and increased leukocyte infiltration.

Solid tumors require stroma for growth beyond a minimal size (47), and we found that poor stroma organization was associated with reduced tumor growth. One possible explanation for this growth reduction is immunologically based, a context in which the role of SPARC has never been investigated previously. Stroma may act as a shield to protect tumors from immune cell infiltration (48) and may participate in processes leading to tumor antigen presentation (49). In the heavily infiltrated N2C tumors from SPARC$^{-/-}$ mice, most of the granulocytes and macrophages were localized within the numerous and large necrotic areas and expressed TNFα and IFNγ; inhibition of these cytokines by neutralizing mAb abrogated the delayed growth of tumors in SPARC$^{-/-}$ mice. These cytokines can kill tumor cells both directly and indirectly through activation of PMNs that interact with tumor cells and endothelial cells for subsequent lysis (50).

A second possibility to explain the impaired tumor growth in SPARC$^{-/-}$ mice is a reduced blood supply because stroma is the area of vessels cooptation (51). Our analysis revealed fewer and smaller blood vessels in tumors from SPARC$^{-/-}$ than SPARC$^{+/+}$ mice, consistent with earlier suggestions (52) and with previous in vitro analyses that correlated SPARC expression with tumor neoangiogenesis (53, 54). Moreover, a reduced number of blood vessels was found in vivo in the capsule surrounding biomaterials implanted in SPARC$^{-/-}$ mice as part of the host reaction to foreign body (55).

Together, our data demonstrate a role for host leukocyte–produced SPARC in determining the structure and function of tumor-associated stroma through the organization of collagen, which in lobular mammary carcinoma, is mainly type IV. Whether facilitated leukocyte infiltration favors tumor-specific immune attack remains to be investigated.

Recently, Brekken et al. (56) reported that the SPARC producer 3LL lung carcinoma cell line and the nonproducer EL-4 lymphoma line grew faster in SPARC$^{-/-}$ mice backcrossed for four generations to B6 than in wild-type B6 mice. This finding is apparently contradictory only because 3LL tumors also had reduced collagen, albeit it was collagen type I whereas type IV was the most affected in our model because of the different histotype. Differences in the prominent type of collagen and its proteolysis can gen-

erate fragments favoring or inhibiting tumor angiogenesis. Indeed, trimer carboxyl propeptide of collagen type I is chemotactic for endothelial cells (57), whereas collagen type IV degradation by MMP-9 generates tumstatin that induces apoptosis of proliferating endothelial cells (58). The tumor growth differences might also rest in possibility that cell lines established over 30 yr of passages (59) are likely less sensitive to environmental factors than primary cell lines. Indeed, N2C carcinomas do not grow when transplanted outside the mammary fat pad (unpublished data), whereas 3LL tumors grow ectopically and even overcome MHC barriers (60).

If diverse histotypes actually underlie differential tumor growth in SPARC$^{-/-}$, further analysis of tumor-derived SPARC seems warranted because it is not clear whether it differs functionally from that of host origin. Our recently obtained mammary cell lines from SPARC$^{-/-}$ mice carrying the mouse mammary tumor virus–HER-2/neu–activated rat oncogene should help to determine the role of tumor-derived SPARC, whereas BMT from SPARC$^{+/+}$ into SPARC$^{-/-}$ neu$^{+/-}$ mice should indicate the role of BM-derived SPARC in the various phases of mammary gland transformation.

We are grateful to Professors I. Hart and A. Mantovani for helpful discussion and critical reading of the manuscript. We thank Dr. C. Melani for protocol development and screening of earlier backcross generations; Dr. C. Chiodoni for help in FACS® analysis; and L. Gioiosa, M. Parenza, and I. Arioli for expert technical assistance.

This work was supported by Associazione Italiana Ricerca sal Cancro, Italian Ministry of Health, and Italian Ministry for University and Scientific and Technological Research. S. Sangaletti is a recipient of a fellowship from the Italian Foundation for Cancer Research.

Submitted: 5 February 2003
Accepted: 22 September 2003

References

1. Balkwill, F., and A. Mantovani. 2001. Inflammation and cancer: back to Virchow? *Lancet.* 17:539–544.
2. Coussens, L.M., and Z. Werb. 2001. Inflammatory cells and cancer: think different! *J. Exp. Med.* 19:23–26.
3. Moore, R., D. Owens, G. Stamp, C. Arnott, F. Burke, N. East, H. Holdsworth, L. Turner, B. Rollins, M. Pasparakis, et al. 1999. Tumour necrosis factor-α deficient mice are resistant to skin carcinogenesis. *Nat. Med.* 5:828–831.
4. Vidal-Vanaclocha, F., G. Fantuzzi, and L. Mendoza. 2000. IL-18 regulates IL-1β-dependent hepatic melanoma metastasis via vascular cell adhesion molecule-1. *Proc. Natl. Acad. Sci. USA.* 97:734–739.
5. Wiktor-Jedrzejczak, W., A. Bartocci, A.W. Ferrante, A. Ahmed-Ansari, K.W. Sell, J.W. Pollard, and E.R. Stanley. 1990. Total absence of colony-stimulating factor 1 in the macrophage-deficient osteopetrotic (op/op) mouse. *Proc. Natl. Acad. Sci. USA.* 87:4828–4832.
6. Yoshida, H., S. Hayashi, T. Kunisada, M. Ogawa, S. Nishikawa, H. Okamura, T. Sudo, L.D. Shultz, and S. Nishikawa. 1990. The murine mutation osteopetrosis is in the coding region of the macrophage colony stimulating factor gene. *Nature.* 31:442–444.
7. Nowicki, A., J. Szenajch, G. Ostrowska, A. Wojtowicz, K. Wojtowicz, A.A. Kruszewski, M. Maruszynski, S.L. Aukerman, and W. Wiktor-Jedrzejczak. 1996. Impaired tumor growth in colony-stimulating factor 1 (CSF-1)-deficient, macrophage-deficient op/op mouse: evidence for a role of CSF-1-dependent macrophages in formation of tumor stroma. *Int. J. Cancer.* 65:112–119.
8. Lin, E.Y., A.V. Nguyen, R.G. Russel, and J.W. Pollard. 2001. Colony-stimulating factor I promotes progression of mammary tumor to malignancy. *J. Exp. Med.* 193:727–740.
9. Coussens, L.M., C.L. Tinkle, D. Hanahan, and Z. Werb. 2000. MMP-9 supplied by bone marrow-derived cells contributes to skin carcinogenesis. *Cell.* 103:481–490.
10. Huang, S., M. Van Arsdall, S. Tedjarati, M. McCarty, W. Wu, R. Langley, and I.J. Fidler. 2002. Contributions of stromal metalloproteinase-9 to angiogenesis and growth of human ovarian carcinoma in mice. *J. Natl. Cancer Inst.* 94:1134–1142.
11. Clezardin, P., L. Malaval, A.S. Ehrensperger, P.D. Delmas, M. Dechavanne, and J.L. McGregor. 1988. Complex formation of human thrombospondin with osteonectin. *Eur. J. Biochem.* 175:275–284.
12. Rosenblatt, S., J.A. Bassuk, C.E. Alpers, E.H. Sage, R. Timpl, and K.T. Preissner. 1997. Differential modulation of cell adhesion by interaction between adhesive and counteradhesive proteins: characterization of the binding of vitronectin to osteonectin (BM40, SPARC). *Biochem. J.* 324:311–319.
13. Mayer, U., M. Aumailley, K. Mann, R. Timpl, and J. Engel. 1991. Calcium-dependent binding of basement membrane protein BM-40 (osteonectin, SPARC) to basement membrane collagen type IV. *Eur. J. Biochem.* 198:141–150.
14. Bradshaw, A.D., and E.H. Sage. 2001. SPARC, a matricellular protein that functions in cellular differentiation and tissue response to injury. *J. Clin. Invest.* 107:1049–1054.
15. Martinek, N., R. Zou, M. Berg, J. Sodek, and M. Ringuette. 2002. Evolutionary conservation and association of SPARC with the basal lamina in *Drosophila. Dev. Genes Evol.* 212: 124–133.
16. Swaroop, A., B.L. Hogan, and U. Francke. 1988. Molecular analysis of the cDNA of human SPARC/osteonectin/BM-40: sequence, expression, and localization of the gene to chromosome 5q31-q33. *Genomics.* 2:37–47.
17. Hasselaar, P., and E.H. Sage. 1992. SPARC antagonizes the effect of bFGF on the migration of bovine aortic endothelial cells. *J. Cell. Biochem.* 49:272–283.
18. Raines, E.W., T.F. Lane, M.L. Iruela-Arispe, R. Ross, and E.H. Sage. 1992. The extracellular glycoprotein SPARC interacts with platelet-derived growth factor (PDGF)-AB and -BB and inhibits the binding of PDGF to its receptors. *Proc. Natl. Acad. Sci. USA.* 89:1281–1285.
19. Kupprion, C., K. Motamed, and E.H. Sage. 1999. SPARC inhibits the mitogenic effect of vascular endothelial growth factor on microvascular endothelial cells. *J. Biol. Chem.* 273: 29635–29640.
20. Delany, A.M., I. Kalajzic, A.D. Bradshaw, E.H. Sage, and E. Canalis. 2003. Osteonectin null mutation compromises osteoblast formation, maturation, and survival. *Endocrinology.* 144:2588–2596.
21. Yan, Q., and E.H. Sage. 1999. SPARC, a matricellular glycoprotein with important biological functions. *J. Histochem. Cytochem.* 47:1495–1506.

22. Colombo, M.P., G. Ferrari, G. Biondi, D. Galasso, C.C. Howe, and G. Parmiani. 1991. SPARC/osteonectin/BM-40 expression in methylcholanthrene-induced fibrosarcomas and in Kirsten-MSV-transformed fibroblasts. *Eur. J. Cancer.* 27: 58–62.
23. Mettouchi, A., F. Cabon, N. Montreau, P. Vernier, G. Mercier, D. Blangy, H. Tricoire, P. Vigier, and B. Binetruy. 1994. SPARC and thrombospondin genes are repressed by the c-jun oncogene in rat embryo fibroblasts. *EMBO J.* 13: 5668–5678.
24. Vial, E., and M. Castellazzi. 2000. Down-regulation of the extracellular matrix protein SPARC in vSrc- and vJun-transformed chick embryo fibroblasts contributes to tumor formation in vivo. *Oncogene.* 19:1772–1782.
25. Ledda, F., A.I. Bravo, S. Adris, L. Bover, J. Mordoh, and O.L. Podhajcer. 1997. Suppression of SPARC expression by antisense RNA abrogates the tumorigenicity of human melanoma cells. *Nat. Med.* 3:171–176.
26. Gilmour, D.T., G.J. Lyon, M.B. Carlton, J.R. Sanes, M.J. Cunningham, J.R. Anderson, B.L. Hogan, M.J. Evans, and W.H. Colledge. 1998. Mice deficient for the secreted glycoprotein SPARC/osteonectin/BM40 develop normally but show severe age-onset cataract formation and disruption of the lens. *EMBO J.* 17:1860–1870.
27. Norose, K., J.I. Clark, N.A. Syed, A. Basu, E. Heber-Katz, E.H. Sage, and C.C. Howe. 1998. SPARC deficiency leads to early-onset cataractogenesis. *Invest. Ophthalmol. Vis. Sci.* 39:2674–2680.
28. Bassuk, J.A., T. Birkebak, J.D. Rothmier, J.M. Clark, A. Bradshaw, P.J. Muchowski, C.C. Howe, J.I. Clark, and E.H. Sage. 1999. Disruption of the *Sparc* locus in mice alters the differentiation of lenticular epithelial cells and leads to cataract formation. *Exp. Eye Res.* 68:321–331.
29. Delany, A.M., M. Amling, M. Priemel, C. Howe, R. Baron, and E. Canalis. 2000. Osteopenia and decreased bone formation in osteonectin-deficient mice. *J. Clin. Invest.* 105:915–923.
30. Yan, Q., J.I. Clark, T.N. Wight, and E.H. Sage. 2002. Alterations in the lens capsule contribute to cataractogenesis in SPARC-null mice. *J. Cell Sci.* 1:11–18.
31. Di Carlo, E., M.G. Diodoro, K. Boggio, A. Modesti, M. Modesti, P. Nanni, G. Forni, and P. Musiani. 1999. Analysis of mammary carcinoma onset and progression in HER2/neu oncogene transgenic mice reveals a lobular origin. *Lab. Invest.* 79:1261–1269.
32. Boggio, K., G. Nicoletti, E. Di Carlo, F. Cavallo, L. Landuzzi L., C. Melani, M. Giovarelli, I. Rossi, C. De Giovanni, P. Nanni, P. Brouchard, S. Wolf, A. Modesti, P. Musiani, P.L. Lollini, M.P. Colombo, and G. Forni. 1998. IL12-mediated prevention of spontaneous mammary adenocarcinoma in HER2/neu transgenic mice. *J. Exp. Med.* 188: 589–596.
33. Stoppacciaro, A., C. Melani, M. Parenza, A. Mastracchio, C. Bassi, C. Baroni, G. Parmiani, and M.P. Colombo. 1993. Regression of an established tumor genetically modified to release granulocyte colony-stimulating factor requires granulocyte–T cell cooperation and T cell–produced interferon γ. *J. Exp. Med.* 78:151–161.
34. Wiseman, B.S., and Z. Werb. 2002. Stromal effects on mammary gland development and breast cancer. *Science.* 296: 1046–1049.
35. Mok, S.C., W.Y. Chan, K.K. Wong, M.G. Muto, and R.S. Berkowitz. 1996. SPARC, an extracellular matrix protein with tumor-suppressing activity in human ovarian epithelial cells. *Oncogene.* 12:1895–1901.
36. Mok, S.C., K.K. Wong, R.K. Chan, C.C. Lau, S.W. Tsao, R.C. Knapp, and R.S. Berkowitz. 1994. Molecular cloning of differentially expressed genes in human epithelial ovarian cancer. *Gynecol. Oncol.* 52:247–252.
37. Yiu, G.K., W.Y. Chan, S.W. Ng, P.S. Chan, K.K. Cheung, R.S. Berkowitz, and S.C. Mok. 2000. SPARC (secreted protein acidic and rich in cysteine) induces apoptosis in ovarian cancer cells. *Am. J. Pathol.* 159:609–612.
38. Dhanesuan, N., J.A. Sharp, T. Blick, J.T. Price, and E.W. Thompson. 2002. Doxycycline-inducible expression of SPARC/osteonectin/BM40 in MDA-MB-231 human breast cancer cells results in growth inhibition**.** *Breast Cancer Res. Treat.* 75:73–85.
39. Rempel, S.A., S. Ge, and J.A. Gutierrez. 1999. SPARC: a potential diagnostic marker of invasive meningiomas. *Clin. Cancer Res.* 5:237–241.
40. Golembieski, W.A., S. Ge, K. Nelson, T. Mikkelsen, and S.A. Rempel. 1999. Increased SPARC expression promotes U87 glioblastoma invasion in vitro. *Int. J. Dev. Neurosci.* 17: 463–472.
41. Schultz, C., N. Lemke, S. Ge, W.A. Golembieski, and S.A. Rempel. 2002. Secreted protein acidic and rich in cysteine promotes glioma invasion and delays tumor growth in vivo. *Cancer Res.* 62:6270–6277.
42. Xia, M., D. Leppert, S.L. Hauser, S.P. Sreedharan, P.J. Nelson, A. Krensky, and E.J. Goetzl. 1996. Stimulus specificity of matrix metalloproteinase dependence of human T cell migration through a model basement membrane. *J. Immunol.* 156:160–167.
43. Leppert, D., E. Waubant, R. Galardy, N. Bunnett, and S.L. Hauser. 1995. T cell gelatinases mediate basement membrane transmigration in vitro. *J. Immunol.* 154:4379–4389.
44. Ratzinger, R.G., P. Stoizner, S. Ebner, M.B. Lutz, G.T. Layton, C. Rainer, R.M. Senior, J.M. Shipley, P. Fritsch, G. Schuler, and N. Romani. 2002. Matrix metalloproteinases 9 and 2 are necessary for the migration of Langerhans cells and dermal dendritic cells from human and murine skin. *J. Immunol.* 168:4361–4371.
45. Francki, A., A.D. Bradshaw, J.A. Bassuk, C.C. Howe, W.G. Couser, and E.H. Sage. 1999. SPARC regulates the expression of collagen Type I and transforming growth factor-β1 in mesangial cells. *J. Biol. Chem.* 274:32145–32152.
46. Hazelbag S.A. Gorter, G.G. Kenter, L. van der Broke, and G. Fleuren. 2000. Transforming growth factor-β1 induces tumor stroma and reduces tumor infiltrate in cervical cancer. *Pathol. Internat.* 50:884–890.
47. Folkman, J. 1985. Tumor angiogenesis. *Adv. Canc. Res.* 43: 175–203.
48. Ganss, R., and D. Hanahan. 1998. Tumor microenvironment can restrict the effectivness of activated antitumor lymphocytes. *Cancer Res.* 58:4673–4681.
49. Spiotto, M.T., P. Yu, D.A. Rowley, M.J. Nishimura, S.C. Meredith, T.F. Gayewski, Y. Fu, and H. Schreiber. 2002. Increasing tumor antigen expression overcomes "ignorance" to solid tumors via crosspresentation by bone marrow-derived stromal cells. *Immunity.* 17:737–747.
50. Di Carlo, E., G. Forni, P.L. Lollini, M.P. Colombo, A. Modesti, and P. Musiani. 2001. The intriguing role of polymorphonuclear neutrophils in antitumor reactions. *Blood.* 97: 339–345.
51. Holash, J., S.J. Wiegand, and G.D. Yancopoulus. 1999. New

model of tumor angiogenesis: dynamic balance between vessel regression and growth mediated by angiopoietins and VEGF. *Oncogene.* 18:5356–5362.
52. Sage, E.H. 1997. Terms of attachment: SPARC and tumorigenesis. *Nat. Med.* 3:144–146.
53. Iruela-Arispe, M.L., P. Hasselaar, and E.H. Sage. 1991. Differential expression of extracellular matrix proteins is correlated with angiogenesis in vitro. *Lab. Invest.* 64:174–186.
54. Vajkoczy, P., M.D. Menger, R. Goldbrunner, S. Ge, T.A. Fong, B. Vollmar, L. Schilling, A. Ullrich, K.P. Hirth, J.C. Tonn, et al. 2000. Targeting angiogenesis inhibits tumor infiltration and expression of the pro-invasive protein SPARC. *Int. J. Cancer.* 87:261–268.
55. Poulakkaien P., A.D. Brashow, T.R. Kyriakides, M. Reed, R. Brekken, T. Wight, P. Bornstein, B. Ratkner, and E.H. Sage. Compromised production of extracellular matrix in mice lacking secreted protein, acidic and rich in cysteine (SPARC) leads to a reduced foreign body reaction to implanted biomaterials. *Am. J. Pathol.* 167:627–635.
56. Brekken R.A., P. Poulakkainen, D.C. Graves, G. Workman, S.R. Lubkin and E.H. Sage. 2003. Enhanced growth of tumors in SPARC null mice is associated with changes in the ECM. *J. Clin. Invest.* 111:487–495.
57. Palmieri, D., L. Carmadella, V. Ulivi, G. Guasco, and P. Manduca. 2000. Trimer carboxyl propeptide of collagen I produced by mature osteoblasts is chemotactic for endothelial cells. *J. Biol. Chem.* 275:32658–32663.
58. Hamano Y., M. Zeisberg, H. Sugimotu, J.C. lively, Y. Maeshima, C. Yang, R.O. Hynes, Z. Werb, A. Sudhakar, and R. Kalluri. Physiological levels of tumstatin, a fragment of collagen type IV α3 chain, are generated by MMP-9 proteolysis and suppress angiogenesis via $\alpha v\beta 3$ integrin. *Cancer Cell.* 3:589–601.
59. Gresser, I., and C. Bourali-Maury. 1972. Inhibition by interferon preparations of a solid malignant tumour and pulmonary metastases in mice. *Nature.* 236:78–79.
60. Isakov, N., M. Feldman, and S. Segal. 1982. An immune response against the alloantigens of the 3LL Lewis lung carcinoma prevents the growth of lung metastases, but not of local allografts. *Invasion Metastasis.* 2:12–32.